Towards Adaptive Soft Robots with Improved Motion Strategies: Strides in Modeling and Control

Lekan Molu

Microsoft Research

New York City, NY 10012

Presented by **Lekan Molu** (Lay-con Mo-lu)

October 31, 2024

Talk Overview

- The principle of morphological computation in nature
  - Morphology: shape, geometry, and mechanical properties.
  - Computation: sensorimotor information transmission among geometrical components.
- Morphology and computation in artificial robots
  - Cosserat Continua and reduced soft robot models.
  - **Reductions**: Structural Lagrangian properties and control.
- Towards real-time strain regulation and control
  - **Simplexity**: Hierarchical and fast versatile control with reduced variables.

Morphology and computation

- Morphology: Emergent behaviors of natural organisms from complex sensorimotor nonlinear mechanical feedback from the environment.
  - Shape affecting behavioral response.
  - Geometrical Arrangement of motors such that processing and perception affect computational characteristics.
  - Mechanical properties that allow the engineering of emergent behaviors via adaptive environmental interaction.
- Computation: The information transformation among the system geometrical units, upon environmental perception, that effect morphological changes in shape and material properties.

MC in vertebrates – a case for soft designs

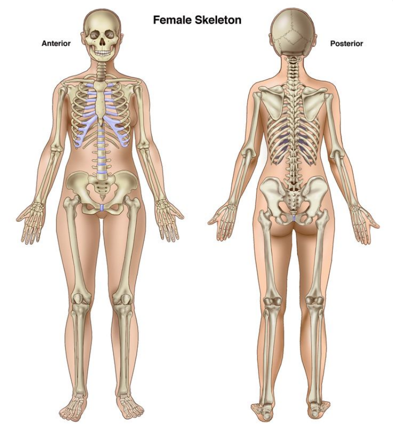

An adult human skeleton $\approxeq 11\%$ of the body mass. ©Brittanica

- The arrangement and compliance of body parts, perception, and computation creates emergence of complex interactive behavior.
- Soft bodies seem critical to the emergence of adaptive natural behaviors.
- Morphological computation is crucial in the design of robots that execute adaptive natural behavior.

Simplexity in Morphological Computation

- Simplexity: Exploiting structure for effective control.
  - The geometrical tuning of the morphology and neural circuitry in the brain of mammals that simplify the perception and control of complex natural phenomena.
  - Not exactly simplified models or reduced complexity.
  - But rather, sparse connections and finite variables to execute adaptive sensorimotor strategies!
- Example: Saccades (focused eye movements) are controlled by (small) Superior Colliculus in the human brain.
  - Plug: Complex neural circuitry; simple control systems!

Simplexity: The Central Pattern Generator

- A neural mechanism (in vertebrates) that generates motor control with minimal parameters.
- CPG: Neurons and synapses couple to generate effective motor activation for rhythmic environmental motion.
  - In Lampreys, only two signals trigger swimming motion, for example!
  - This CPG enables indirect use of brain computational power via nonlinear feedback from stretch receptor neurons on Lamprey's skin.

Saccades and the Superior Colliculus

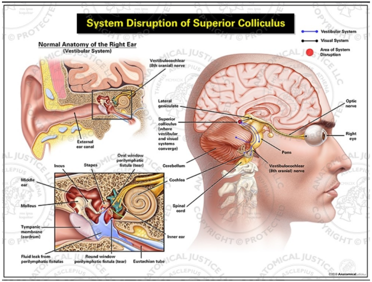

©Anatomical Justice.

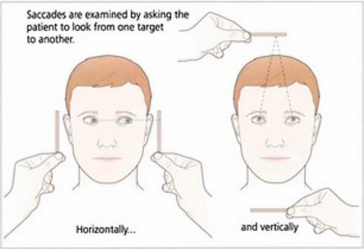

Credit: Vision and Learning Center.

Morphing in Invertebrates: Cephalopods

Cuttlefish. ©Monterey Bay Museum

Octopus. ©Smithsonian Magazine

The Octopus and Cuttlefish

- No exoskeleton, or spinal cord.
- A muscular hydrostat: transversal, longitudinal, and oblique muscles along richly innervated arms and mechanoreceptors:
  - Allows for bending, stretching, stiffening, and retraction.
  - Diverse compliance across eight arms imply sophisticated motion strategies in the wild!
- Simplexity enhanced by a peripheral nervous system and a central nervous system.

Soft Robot Mechanism in Focus

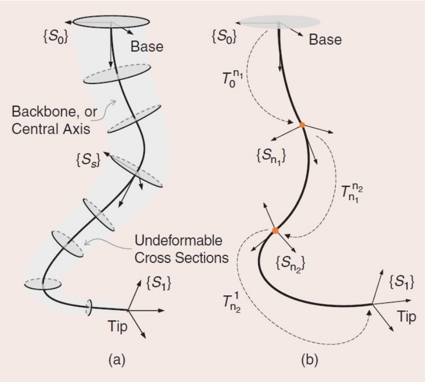

A continuum soft robot whose mechanics can be well-described with Cosserat rod theory. Reprinted from (Della Santina et al. (2023))

- One dimension is quintessentially longer than the other two.
- Characterized by a central axis with undeformable discs that characterize deformable cross-sectional segments.
- Strain and deformation, via e.g. Cosserat rod theory, enables precise finite-dimensional mathematical models.

A Finite and Reliable Model

- A soft robot's usefulness is informed by control system that melds its body deformation with internal actuators.
- By design, this calls for a high-fidelity model or a delicate balancing of complex morphology and data-driven methods.

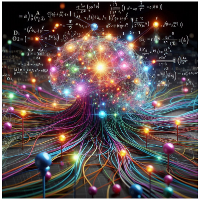

- Non-interpretable; non-reliable.
- $\times$Continuous coupled interaction between the material, actuators, and external affordances.

The case for model-based control

- Soft robots are infinite degrees-of-freedom continua i.e., PDEs are the main tools for analysis.
- Nonlinear PDE theory is tedious and computationally intensive.
- Notable strides in reduced-order, finite-dimensional mathematical models that induce tractability in continuum models.

Tractable reduced-order models

- Morphoelastic filament theory: Moulton et al. (2020); Kaczmarski et al. (2023); Gazzola et al. (2018);
- Generalized Cosserat rod theory: Rubin (2000); Cosserat and Cosserat (1909);
- The constant curvature model: Godage et al. (2011);
- The piecewise constant curvature model: Webster and Jones (2010); Qiu et al. (2023); and
- Ordinary differential equations-based discrete Cosserat model: Renda et al. (2016, 2018).

Cosserat-based piecewise constant strain model

- A discrete Cosserat model: Renda et al. (2018).
  - Shapes defined by a finite-dimensional functional space, parameterized by a curve, $X : [0, L]$..
  - Assumes constant strains between finite nodal points on robot's body.
  - Strain-parameterized dynamics on a reduced special Euclidean-3 group (SE(3)).

The piecewise constant strain model

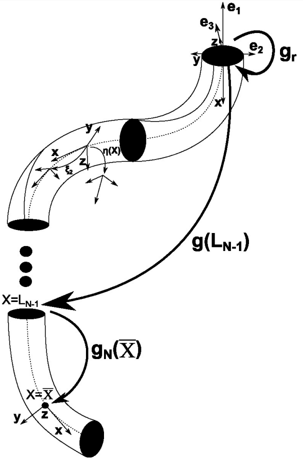

Credit: Renda et al. (2018).

- C-space: $g(X) : X \to \mathbb{SE}(3) = \begin{pmatrix} \boldsymbol{R}(X) & \boldsymbol{p}(X) \\ 0^\top & 1 \end{pmatrix}$.
- Strain and twist vectors: $\{\boldsymbol{\eta}, \boldsymbol{\xi}\} \in \mathbb{R}^6$.
  - $\{\boldsymbol{\eta}, \boldsymbol{\xi}\} := \{\boldsymbol{q}, \dot{\boldsymbol{q}}\}$
- Strain field: $\breve{\boldsymbol{\eta}}(X) = g^{-1}\partial g/\partial X$.
- Twist field: $\breve{\boldsymbol{\xi}}(X) = g^{-1}\partial g/\partial t$.

Dynamic equations

From the continuum equations for a cable-driven soft arm [Renda et al. (2014)], we can derive the following dynamic equation [Renda et al. (2018)]:

$$\underbrace{\left[\int_0^{L_N} J^T \mathcal{M}_a \boldsymbol{J} dX\right]}_{\boldsymbol{M}(\boldsymbol{q})} \ddot{\boldsymbol{q}} + \underbrace{\left[\int_0^{L_N} \boldsymbol{J}^T \text{ad}^{\star}_{\boldsymbol{J}\dot{\boldsymbol{q}}} \mathcal{M}_a \boldsymbol{J} dX\right]}_{\boldsymbol{C}_1(\boldsymbol{q},\dot{\boldsymbol{q}})} \dot{\boldsymbol{q}} + \underbrace{\left[\int_0^{L_N} J^T \mathcal{M}_a \dot{\boldsymbol{J}} dX\right]}_{\boldsymbol{C}_2(\boldsymbol{q},\dot{\boldsymbol{q}})} \dot{\boldsymbol{q}}$$

$$+ \underbrace{\left[\int_0^{L_N} \boldsymbol{J}^T \mathcal{D} \boldsymbol{J} \|\boldsymbol{J}\dot{\boldsymbol{q}}\|_p dX\right]}_{D(\boldsymbol{q},\dot{\boldsymbol{q}})} \dot{\boldsymbol{q}} - \underbrace{(1-\rho_f/\rho)\left[\int_0^{L_N} \boldsymbol{J}^T \mathcal{M} \text{Ad}_{\boldsymbol{g}}^{-1} dX\right] \text{Ad}_{\boldsymbol{g}_r}^{-1} \mathcal{G}}_{\boldsymbol{N}(\boldsymbol{q})}$$

$$- \underbrace{\boldsymbol{J}(\bar{X})^T \mathcal{F}_p}_{\boldsymbol{F}(\boldsymbol{q})} - \underbrace{\int_0^{L_N} \boldsymbol{J}^T \left[\nabla_x \mathcal{F}_i - \nabla_x \mathcal{F}_a + \text{ad}^{\star}_{\boldsymbol{\xi}_n} (\mathcal{F}_i - \mathcal{F}_a)\right] dX}_{\boldsymbol{\tau}(\boldsymbol{q})} = 0, \qquad (1)$$

Structural properties – mass inertia operator

$$\boldsymbol{M}(\boldsymbol{q})\ddot{\boldsymbol{q}} + \left[\boldsymbol{C}_1(q, \dot{\boldsymbol{q}}) + \boldsymbol{C}_2(\boldsymbol{q}, \dot{\boldsymbol{q}})\right]\dot{\boldsymbol{q}} = \boldsymbol{F}(\boldsymbol{q}) + \boldsymbol{N}(\boldsymbol{q})\text{Ad}_{g_r}^{-1}\mathcal{G} + \tau(\boldsymbol{q}) - \boldsymbol{D}(\boldsymbol{q}, \dot{\boldsymbol{q}})\dot{\boldsymbol{q}}. \tag{2}$$

Property 1 (Boundedness of the Mass Matrix)

The mass inertial matrix $\boldsymbol{M}(\boldsymbol{q})$ is uniformly bounded from below by $m\boldsymbol{I}$ where m is a positive constant and $\boldsymbol{I}$ is the identity matrix.

Proof of Property 1.

This is a restatement of the lower boundedness of $\boldsymbol{M}(\boldsymbol{q})$ for fully actuated n-degrees of freedom manipulators [Romero et al. (2014)]. □

Structural properties – parameters Identification

Property 2 (Linearity-in-the-parameters)

There exists a constant vector $\boldsymbol{\Theta} \in \mathbb{R}^{l}$ *and a regressor function* $Y(\boldsymbol{q}, \dot{\boldsymbol{q}}, \ddot{\boldsymbol{q}}) \in \mathbb{R}^{N \times l}$ *such that*

$$M(\boldsymbol{q})\ddot{(\boldsymbol{q})} + \left[C_1(\boldsymbol{q}, \dot{\boldsymbol{q}}) + C_2(\boldsymbol{q}, \dot{\boldsymbol{q}}) + D(\boldsymbol{q}, \dot{\boldsymbol{q}})\right] \dot{\boldsymbol{q}} - \boldsymbol{F}(\boldsymbol{q})N(\boldsymbol{q})Ad_{g_r}^{-1}\mathcal{G} = \boldsymbol{Y}(\boldsymbol{q}, \dot{\boldsymbol{q}}, \ddot{\boldsymbol{q}})\Theta. \tag{3}$$

Structural properties – skew symmetry of system inertial forces

Property 3 (Skew symmetric property)

The matrix $\dot{M}(\boldsymbol{q}) - 2\left[C_1(\boldsymbol{q}, \dot{\boldsymbol{q}}) + C_2(\boldsymbol{q}, \dot{\boldsymbol{q}})\right]$ *is skew-symmetric.*

Skew-symmetric of robot's mass and Coriolis forces

By Leibniz's rule, we have

$$\dot{\boldsymbol{M}}(\boldsymbol{q}) = \frac{d}{dt}\left(\int_0^{L_N} \boldsymbol{J}^T \mathcal{M}_a \boldsymbol{J} dX\right) = \int_0^{L_N} \frac{\partial}{\partial t}\left(\boldsymbol{J}^T \mathcal{M}_a \boldsymbol{J}\right) dX$$
$$\triangleq \int_0^{L_N} \left(\dot{\boldsymbol{J}}^T \mathcal{M}_a \boldsymbol{J} + \boldsymbol{J}^T \dot{\mathcal{M}}_a \boldsymbol{J} + \boldsymbol{J}^T \mathcal{M}_a \dot{\boldsymbol{J}}\right) dX. \tag{4}$$

Therefore, $\dot{\boldsymbol{M}}(\boldsymbol{q}) - 2\left[C_1(\boldsymbol{q}, \dot{\boldsymbol{q}}) + C_2(\boldsymbol{q}, \dot{\boldsymbol{q}})\right]$ becomes

$$\int_0^{L_N} \left(\dot{\boldsymbol{J}}^\top \mathcal{M}_a \boldsymbol{J} + \boldsymbol{J}^\top \dot{\mathcal{M}}_a \boldsymbol{J} + \boldsymbol{J}^\top \mathcal{M}_a \dot{\boldsymbol{J}}\right) dX - 2\int_0^{L_N} \left(\boldsymbol{J}^\top \text{ad}^\star_{\boldsymbol{J}\dot{\boldsymbol{q}}} \mathcal{M}_a \boldsymbol{J} + \boldsymbol{J}^\top \mathcal{M}_a \dot{\boldsymbol{J}}\right) dX \tag{5}$$

$$\triangleq \int_0^{L_N} \left(\dot{\boldsymbol{J}}^\top \mathcal{M}_a \boldsymbol{J} + \boldsymbol{J}^\top \dot{\mathcal{M}}_a \boldsymbol{J} - \boldsymbol{J}^\top \mathcal{M}_a \dot{\boldsymbol{J}}\right) dX - 2\int_0^{L_N} \boldsymbol{J}^\top \text{ad}^\star_{\boldsymbol{J}\dot{\boldsymbol{q}}} \mathcal{M}_a \boldsymbol{J} dX. \tag{6}$$

Skew-Symmetric Property Proof

Similarly, $-\left[\dot{\boldsymbol{M}}(\boldsymbol{q}) - 2\left[\boldsymbol{C}_1(\boldsymbol{q},\dot{\boldsymbol{q}}) + \boldsymbol{C}_2(\boldsymbol{q},\dot{\boldsymbol{q}})\right]\right]^\top$ expands as

$$
\begin{aligned}
&-\dot{\boldsymbol{M}}^\top(\boldsymbol{q}) + 2\left[\boldsymbol{C}_1^\top(\boldsymbol{q},\dot{\boldsymbol{q}}) + \boldsymbol{C}_2^\top(\boldsymbol{q},\dot{\boldsymbol{q}})\right] = \\
&\int_0^{L_N} dX^\top \left(-\boldsymbol{J}^\top \mathcal{M}_a \dot{\boldsymbol{J}} - \boldsymbol{J}^\top \dot{\mathcal{M}}_a \boldsymbol{J} - \dot{\boldsymbol{J}}^\top \mathcal{M}_a \boldsymbol{J}\right) + 2\int_0^{L_N} dX^\top \left(\boldsymbol{J}^\top \mathcal{M}_a \mathrm{ad}_{\boldsymbol{J}\dot{\boldsymbol{q}}} \boldsymbol{J} + \dot{\boldsymbol{J}}^\top \mathcal{M}_a \boldsymbol{J}\right) \\
&\triangleq \int_0^{L_N} \left(\boldsymbol{J}^\top \mathcal{M}_a \dot{\boldsymbol{J}} - \dot{\boldsymbol{J}}^\top \mathcal{M}_a \boldsymbol{J} - \boldsymbol{J}^\top \dot{\mathcal{M}}_a \boldsymbol{J}\right) dX - 2\int_0^{L_N} J^\top \mathrm{ad}^\star_{\boldsymbol{J}\dot{\boldsymbol{q}}} \mathcal{M}_a \boldsymbol{J} dX \qquad (7)
\end{aligned}
$$

which satisfies the identity:

$$
\begin{aligned}
\dot{\boldsymbol{M}}(\boldsymbol{q}) - 2\left[\boldsymbol{C}_1(\boldsymbol{q},\dot{\boldsymbol{q}}) + \boldsymbol{C}_2(\boldsymbol{q},\dot{\boldsymbol{q}})\right] = \\
-\left[\dot{\boldsymbol{M}}(\boldsymbol{q}) - 2\left[\boldsymbol{C}_1(\boldsymbol{q},\dot{\boldsymbol{q}}) + \boldsymbol{C}_2(\boldsymbol{q},\dot{\boldsymbol{q}})\right]\right]^\top . \qquad (8)
\end{aligned}
$$

A fortiori, the skew symmetric property follows.

MC Takeaways: Simplexity

- Simplexity: Reliance on a few parameters to model an infinite-DoF system:

$$\boldsymbol{M}(\boldsymbol{q})\ddot{\boldsymbol{q}} + \left[\boldsymbol{C}_1(\boldsymbol{q}, \dot{\boldsymbol{q}}) + \boldsymbol{C}_2(\boldsymbol{q}, \dot{\boldsymbol{q}})\right]\dot{\boldsymbol{q}} = \boldsymbol{F}(\boldsymbol{q}) + \boldsymbol{N}(\boldsymbol{q})\mathrm{Ad}_{\boldsymbol{g}_r}^{-1}\mathcal{G} + \tau(\boldsymbol{q}) - \boldsymbol{D}(\boldsymbol{q}, \dot{\boldsymbol{q}})\dot{\boldsymbol{q}}.$$

- Simplexity: From PDE to ODE, i.e. inifinite-dimensional analysis (Continuum PDE) to finite-dimensional ODE!

Control exploiting structural properties

Regarding the generalized torque $\boldsymbol{\tau}(\boldsymbol{q})$ as a control input, $\boldsymbol{u}(\boldsymbol{q}, \dot{\boldsymbol{q}})$, feedback laws are sufficient for attaining a desired soft body configuration.

Theorem 1 (Cable-driven Actuation)

For positive definite diagonal matrix gains $\boldsymbol{K}_D$ and $\boldsymbol{K}_p$, without gravity/buoyancy compensation, the control law

$$\boldsymbol{u}(\boldsymbol{q}, \dot{\boldsymbol{q}}) = -\boldsymbol{K}_p \tilde{\boldsymbol{q}} - \boldsymbol{K}_D \dot{\boldsymbol{q}} - \boldsymbol{F}(\boldsymbol{q}) \tag{9}$$

under a cable-driven actuation globally asymptotically stabilizes system (2), where $\tilde{\boldsymbol{q}}(t) = \boldsymbol{q}(t) - \boldsymbol{q}^d$ is the joint error vector for a desired equilibrium point $\boldsymbol{q}^d$.

Computational Control exploiting structural properties

Corollary 2 (Fluid-driven actuation)

If the robot is operated without cables, and is driven with a dense medium such as pressurized air or water, then the term $F(\boldsymbol{q}) = 0$ *so that the control law* $\boldsymbol{u}(\boldsymbol{q}, \dot{\boldsymbol{q}}) = -\boldsymbol{K}_p \tilde{\boldsymbol{q}} - \boldsymbol{K}_D \dot{\boldsymbol{q}}$ *globally asymptotically stabilizes the system.*

Proof.

Proofs in Section V of Molu and Chen (2024). □

Robot parameters

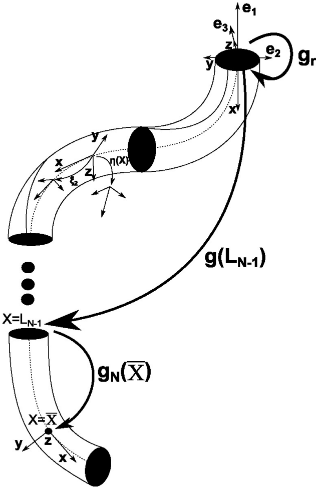

- Tip load in the $+y$ direction in the robot's base frame.
- Poisson ratio: 0.45; $\mathcal{M} = \rho[I_x, I_y, I_z, A, A, A]$ with $\rho = 2,000 kgm^{-3}$;
- $\boldsymbol{D} = -\rho_w \nu^T \nu \check{\boldsymbol{D}} \nu / |\nu|$.
- $X \in [0, L]$ discretized into 41 segments.

Computational Control exploiting structural properties

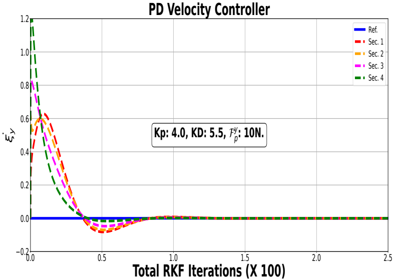

Cable-driven, strain twist setpoint terrestrial control.

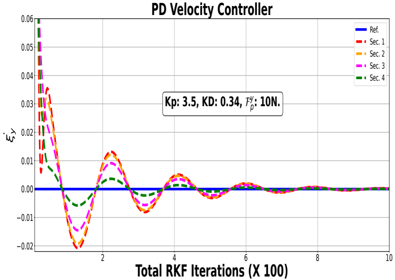

Fluid-actuated, strain twist setpoint terrestrial control.

Computational Control exploiting structural properties

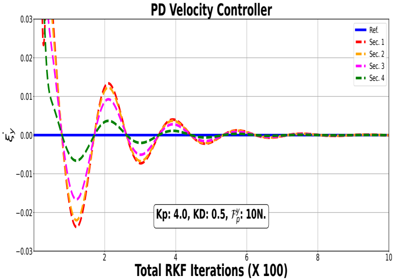

Fluid-actuated, strain twist setpoint underwater control.

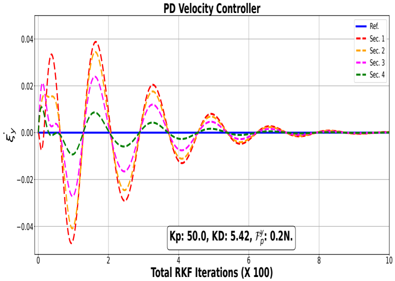

Cable-driven, strain twist setpoint regulation.

Computational Control exploiting structural properties

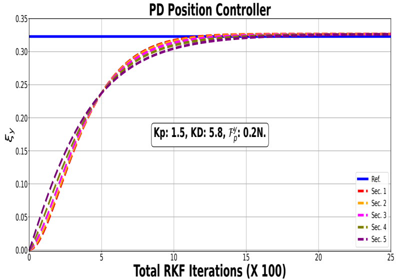

Cable-based position control with a small tip load, 0.2N.

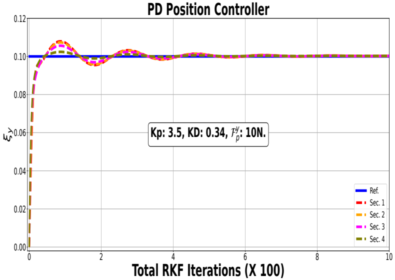

Terrestrial position control.

Exploiting Mechanical Nonlinearity for Feedback!

This page is left blank intentionally.

Hierarchical Dynamics and Control

- Reaching steps towards the real-time strain control of multiphysics, multiscale continuum soft robots.
- Separate subdynamics — aided by a perturbing time-scale separation parameter.
- Respective stabilizing nonlinear backstepping controllers.
- Stability of the interconnected singularly perturbed. system.
- Fast numerical results on a single arm of the Octopus robot arm.

A case for layered control

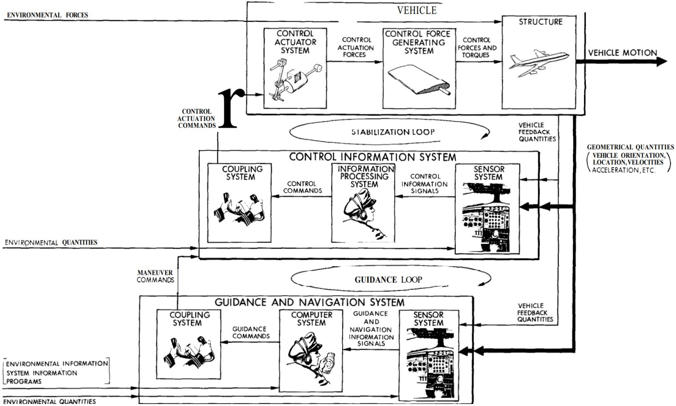

©C. Draper, "Guidance and Navigation, MIT, 1965.

Layered control architecture: Singularly Perturbed Dynamics

- Essentially a layered multirate control scheme (Matni et al. (2024)) of the various interconnected physics components of a soft robot prototype.
- Informed by a standard two-time-scale singularly perturbed system.

$$\dot{\boldsymbol{z}}_1 = \boldsymbol{f}(\boldsymbol{z}_1, \boldsymbol{z}_2, \epsilon, \boldsymbol{u}_s, t), \;\; \boldsymbol{z}_1(t_0) = \boldsymbol{z}_1(0), \;\; \boldsymbol{z}_1 \in \mathbb{R}^{6N}, \tag{10a}$$

$$\epsilon\dot{\boldsymbol{z}}_2 = \boldsymbol{g}(\boldsymbol{z}_1, \boldsymbol{z}_2, \epsilon, \boldsymbol{u}_f, t), \;\; \boldsymbol{z}_2(t_0) = \boldsymbol{z}_2(0), \;\; \boldsymbol{z}_2 \in \mathbb{R}^{6N} \tag{10b}$$

Framework: Singularly Perturbed Dynamics

- $\boldsymbol{f}$ and $\boldsymbol{g}$ are $\mathcal{C}^n(n \gg 0)$ differentiable functions of their arguments;
- $\epsilon > 0$ denotes all small parameters to be ignored.
- $\boldsymbol{u}_s$ is the slow sub-dynamics' control law, and
- $\boldsymbol{u}_f$ is the fast sub-dynamics' controller.

Isolated Equilibrium Manifold Justification

Assumption 1 (Real and distinct root)

Equation (10) has the unique and distinct root $\boldsymbol{z}_2 = \phi(\boldsymbol{z}_1, t)$ *(for a sufficiently smooth* ϕ*) so that*

$$0 = \boldsymbol{g}(\boldsymbol{z}_1, \phi(\boldsymbol{z}_1, t), 0, 0, t) \triangleq \bar{\boldsymbol{g}}(\boldsymbol{z}_1, 0, t), \;\; \boldsymbol{z}_1(t_0) = \boldsymbol{z}_1(0). \tag{11}$$

The slow subsystem therefore becomes

$$\dot{\boldsymbol{z}}_1 = \boldsymbol{f}(\boldsymbol{z}_1, \phi(\boldsymbol{z}_1, t), 0, \boldsymbol{u}_s, t) \triangleq \boldsymbol{f}_s(\boldsymbol{z}_1, \boldsymbol{u}_s, t). \tag{12}$$

Framework: Slow Dynamics Extraction

- Assumption: the fast feedback law is asymptotically stable;
  - It does not modify the open-loop equilibrium manifold of the fast dynamics.
- With $\epsilon = 0$ we have,

$$\dot{\boldsymbol{z}}_1 = \boldsymbol{f}(\boldsymbol{z}_1, \boldsymbol{z}_2, 0, \boldsymbol{u}_s, t), \;\; \boldsymbol{z}_1(t_0) = \boldsymbol{z}_1(0), \tag{13a}$$

$$0 = \boldsymbol{g}(\boldsymbol{z}_1, \boldsymbol{z}_2, 0, 0, t). \tag{13b}$$

Framework: Fast Dynamics Extraction

Introduce the time scale $T = t/\epsilon$, and write the deviation of $\boldsymbol{z}_2$ from its isolated equilibrium manifold, $\phi(\boldsymbol{z}_1, t)$ as $\tilde{\boldsymbol{z}}_2 = \boldsymbol{z}_2 - \phi(\boldsymbol{z}_1, t)$. Then, (10) becomes

$$\frac{d\boldsymbol{z}_1}{dT} = \epsilon \boldsymbol{f}\left(\boldsymbol{z}_1, \tilde{\boldsymbol{z}}_2 + \phi(\boldsymbol{z}_1, t), \epsilon, \boldsymbol{u}_s, t\right), \tag{14a}$$

$$\frac{d\tilde{\boldsymbol{z}}_2}{dT} = \epsilon \frac{d\boldsymbol{z}_2}{dt} - \epsilon \frac{\partial \phi}{\partial \boldsymbol{z}_1} \dot{\boldsymbol{z}}_1, \tag{14b}$$

$$= \boldsymbol{g}\left(\boldsymbol{z}_1, \tilde{\boldsymbol{z}}_2 + \phi(\boldsymbol{z}_1, t), \epsilon, \boldsymbol{u}_f, t\right) - \epsilon \frac{\partial \phi(\boldsymbol{z}_1, t)}{\partial \boldsymbol{z}_1} \dot{\boldsymbol{z}}_1. \tag{14c}$$

Framework for singularly perturbed dynamics

Setting $\epsilon = 0$, we obtain the algebraic equation

$$\frac{d\tilde{\boldsymbol{z}}_2}{dT} = \boldsymbol{g}(\boldsymbol{z}_1, \tilde{\boldsymbol{z}}_2 + \phi(z_1, t), 0, \boldsymbol{u}_f, t) \tag{15}$$

with $\boldsymbol{z}_1$ frozen to its initial values.

Decomposition of SoRo Rod Dynamics

This page is left blank intentionally

Decomposition of SoRo Rod Dynamics

- $\mathcal{M}_i^{\text{core}}$: composite mass distribution as a result of microsolid i's barycenter motion;
- $\mathcal{M}^{\text{pert}}$: motions relative to $\mathcal{M}_i^{\text{core}}$, considered as a perturbation;
- $\mathcal{M} = \mathcal{M}^{\text{pert}} \cup \mathcal{M}^{\text{core}}$.
- Introduce the transformation: $[\boldsymbol{q}, \dot{\boldsymbol{q}}] = [\boldsymbol{q}, \boldsymbol{z}]$, rewrite (2):

$$\boldsymbol{M}(\boldsymbol{q})\dot{\boldsymbol{z}} + [\boldsymbol{C}_1(\boldsymbol{q}, \boldsymbol{z}) + \boldsymbol{C}_2(\boldsymbol{q}, \boldsymbol{z}) + \boldsymbol{D}(\boldsymbol{q}, \boldsymbol{z})]\, \boldsymbol{z} - \boldsymbol{F}(\boldsymbol{q}) - \boldsymbol{N}(\boldsymbol{q})\text{Ad}_{g_r}^{-1}\mathcal{G} = \tau(\boldsymbol{q})$$

Dynamics separation

Suppose that $\boldsymbol{M}^p = \int_{L^p_{\min}}^{L^p_{\max}} \boldsymbol{J}^\top \boldsymbol{\mathcal{M}}^{pert} \boldsymbol{J} dX$, and $\boldsymbol{M}^c = \int_{L^c_{\min}}^{L^c_{\max}} \boldsymbol{J}^\top \mathcal{M}^{core} \boldsymbol{J} dX$, then,

$$\boldsymbol{M}(\boldsymbol{q}) = (\boldsymbol{M}^c + \boldsymbol{M}^p)(\boldsymbol{q}), \; \boldsymbol{N} = (\boldsymbol{N}^c + \boldsymbol{N}^p)(\boldsymbol{q}), \tag{16a}$$

$$\boldsymbol{F}(\boldsymbol{q}) = (\boldsymbol{F}^c + \boldsymbol{F}^p)(\boldsymbol{q}), \quad \boldsymbol{D}(\boldsymbol{q}) = (\boldsymbol{D}^c + \boldsymbol{D}^p)(\boldsymbol{q}) \tag{16b}$$

$$\boldsymbol{C}_1(\boldsymbol{q}, \dot{\boldsymbol{q}}) = (\boldsymbol{C}_1^c + \boldsymbol{C}_1^p)(\boldsymbol{q}, \dot{\boldsymbol{q}}), \tag{16c}$$

$$\boldsymbol{C}_2(\boldsymbol{q}, \dot{\boldsymbol{q}}) = (\boldsymbol{C}_2^c + \boldsymbol{C}_2^p)(\boldsymbol{q}, \dot{\boldsymbol{q}}). \tag{16d}$$

Dynamics Separation

Furthermore, let

$$M = \underbrace{\begin{bmatrix} \mathcal{H} & \mathbf{0} \\ \mathbf{0} & \mathbf{0} \end{bmatrix}}_{M^c(\boldsymbol{q})} + \underbrace{\begin{bmatrix} \mathbf{0} & \mathcal{H}_{\text{slow}}^{\text{fast}} \\ \mathcal{H}_{\text{slow}}^{\text{fast}\,\top} & \mathcal{H}_{\text{slow}} \end{bmatrix}}_{M^p(\boldsymbol{q})}, \tag{17}$$

where $\mathcal{H}_{\text{slow}}^{\text{fast}}$ denotes the decomposed mass of the perturbed sections of the robot relative to the core sections.

- Let robot's state, $\boldsymbol{x} = [\boldsymbol{q}^\top, \boldsymbol{z}^\top]^\top$ decompose as $\boldsymbol{q} = [\boldsymbol{q}_{\text{fast}}^\top, \boldsymbol{q}_{\text{slow}}^\top]^\top$ and $\boldsymbol{z} = [\boldsymbol{z}_{\text{fast}}^\top, \boldsymbol{z}_{\text{slow}}^\top]^\top$,
- Define $\bar{M}^p = M^p/\epsilon$, and let $\boldsymbol{u} = [\boldsymbol{u}_{\text{fast}}^\top, \boldsymbol{u}_{\text{slow}}^\top]^\top$ be the applied torque.

SoRo Dynamics Separation

$$(\boldsymbol{M}^c + \epsilon \bar{\boldsymbol{M}}^p)\dot{\boldsymbol{z}} = \boldsymbol{s} + \boldsymbol{u}, \tag{18}$$

where

$$\boldsymbol{s} = \begin{bmatrix} \boldsymbol{s}_{\text{fast}} \\ \boldsymbol{s}_{\text{slow}} \end{bmatrix} = \begin{bmatrix} \boldsymbol{F}^c + \boldsymbol{N}^c \text{Ad}_{\boldsymbol{g}_r}^{-1} \boldsymbol{\mathcal{G}} - [\boldsymbol{C}_1^c + \boldsymbol{C}_2^c + \boldsymbol{D}^c]\boldsymbol{z}_{\text{fast}} \\ \boldsymbol{F}^p + \boldsymbol{N}^p \text{Ad}_{\boldsymbol{g}_r}^{-1} \boldsymbol{\mathcal{G}} - [\boldsymbol{C}_1^p + \boldsymbol{C}_2^p + \boldsymbol{D}^p]\boldsymbol{z}_{\text{slow}} \end{bmatrix}. \tag{19}$$

- Since $\boldsymbol{\mathcal{H}}_{\text{fast}}$ is invertible, let

$$\bar{\boldsymbol{M}}^p = \begin{bmatrix} \bar{\boldsymbol{M}}_{11}^p & \bar{\boldsymbol{M}}_{12}^p \\ \bar{\boldsymbol{M}}_{21}^p & \bar{\boldsymbol{M}}_{22}^p \end{bmatrix} \text{ and } \boldsymbol{\Delta} = \begin{bmatrix} \boldsymbol{0} & \boldsymbol{0} \\ \bar{\boldsymbol{M}}_{21}^p \boldsymbol{\mathcal{H}}_{\text{fast}}^{-1} & \boldsymbol{0} \end{bmatrix}. \tag{20}$$

SoRo Dynamics Separation

Premultiplying both sides by $\boldsymbol{I} - \epsilon\boldsymbol{\Delta}$, it can be verified that

$$\begin{bmatrix} \boldsymbol{\mathcal{H}}_{\text{fast}} & \bar{\boldsymbol{M}}_{12}^{p} \\ \boldsymbol{0} & \bar{\boldsymbol{M}}_{22}^{p} \end{bmatrix} \begin{bmatrix} \dot{\boldsymbol{z}}_{\text{fast}} \\ \epsilon \dot{\boldsymbol{z}}_{\text{slow}} \end{bmatrix} = \begin{bmatrix} \boldsymbol{s}_{\text{fast}} \\ \boldsymbol{s}_{\text{slow}} - \epsilon \bar{\boldsymbol{M}}_{21}^{p} \boldsymbol{\mathcal{H}}_{\text{fast}}^{-1} \boldsymbol{s}_{\text{fast}} \end{bmatrix} + \begin{bmatrix} \boldsymbol{u}_{\text{fast}} \\ \boldsymbol{u}_{\text{slow}} - \epsilon \bar{\boldsymbol{M}}_{21}^{p} \boldsymbol{\mathcal{H}}_{\text{fast}}^{-1} \boldsymbol{u}_{\text{fast}} \end{bmatrix} \tag{21}$$

which is in the standard singularly perturbed form (10):

$$\dot{\boldsymbol{z}}_1 = \boldsymbol{f}(\boldsymbol{z}_1, \boldsymbol{z}_2, \epsilon, \boldsymbol{u}_s, t), \;\; \boldsymbol{z}_1(t_0) = \boldsymbol{z}_1(0), \;\; \boldsymbol{z}_1 \in \mathbb{R}^{6N}, \tag{22a}$$

$$\epsilon \dot{\boldsymbol{z}}_2 = \boldsymbol{g}(\boldsymbol{z}_1, \boldsymbol{z}_2, \epsilon, \boldsymbol{u}_f, t), \;\; \boldsymbol{z}_2(t_0) = \boldsymbol{z}_2(0), \;\; \boldsymbol{z}_2 \in \mathbb{R}^{6N} \tag{22b}$$

SoRo Fast Subsystem Extraction

On the fast time scale $T = t/\epsilon$, with $dT/dt = 1/\epsilon$ so that,

$$\dot{\boldsymbol{z}}_{\text{fast}} = \frac{d\boldsymbol{z}_{\text{fast}}}{dt} \equiv \frac{1}{\epsilon}\frac{d\boldsymbol{z}_{\text{fast}}}{dT} \triangleq \frac{1}{\epsilon}\boldsymbol{z}'_{\text{fast}}$$

; and

$$\epsilon \dot{\boldsymbol{z}}_{\text{slow}} = \boldsymbol{z}'_{\text{slow}}.$$

Fast subdynamics:

$$\boldsymbol{z}'_{\text{fast}} = \epsilon \mathcal{H}_{\text{fast}}^{-1}(\boldsymbol{s}_{\text{fast}} + \boldsymbol{u}_{\text{fast}}) - \mathcal{H}_{\text{fast}}^{-1}\mathcal{H}_{\text{slow}}^{\text{fast}}\boldsymbol{z}'_{\text{slow}}, \tag{23a}$$

$$\boldsymbol{z}'_{\text{slow}} = \mathcal{H}_{\text{slow}}^{-1}(\boldsymbol{s}_{\text{slow}} - \boldsymbol{u}_{\text{slow}}) - \mathcal{H}_{\text{fast}}^{-1}(\boldsymbol{s}_{\text{fast}} - \boldsymbol{u}_{\text{fast}}) \tag{23b}$$

where the slow variables are frozen on this fast time scale.

SoRo Slow Subsystem Extraction

- We let $\epsilon \to 0$ in (21), so that what is left, i.e.,

$$\dot{\boldsymbol{z}}_{\text{slow}} = \mathcal{H}_{\text{slow}}^{-1}(\boldsymbol{s}_{\text{slow}} + \boldsymbol{u}_{\text{slow}}) \tag{24}$$

constitutes the system's slow dynamics; where the fast components are frozen on this slow time scale.

This page is left blank intentionally

Control of the Fast Strain Subdynamics

- Consider the transformation: $\begin{bmatrix} \theta \\ \phi \end{bmatrix} = \begin{bmatrix} \boldsymbol{q}_{\text{fast}} \\ \boldsymbol{z}_{\text{fast}} \end{bmatrix}$ so that $\theta' = \epsilon \boldsymbol{z}_{\text{fast}} \triangleq \boldsymbol{\nu} :=$ A virtual input.
- Let $\{\boldsymbol{q}^d_{\text{fast}}, \dot{\boldsymbol{q}}^d_{\text{fast}}\} = \{\xi^d_1, \ldots, \xi^d_{n_\xi}, \eta^d_1, \ldots, \eta^d_{n_\xi}\}_{\text{fast}}$ be the desired joint space configuration for the fast subsystem.

Theorem 3 (Molu (2024))

The control law

$$\boldsymbol{u}_{fpos} = \boldsymbol{q}^d_{fast}(t_f) - \boldsymbol{q}_{fast}(t_f) + \boldsymbol{q}'^d_{fast}(t_f)$$

is sufficient to guarantee an exponential stability of the origin of $\theta' = \boldsymbol{\nu}$ such that for all $t_f \geq 0$, $\boldsymbol{q}_{fast}(t_f) \in S$ for a compact set $S \subset \mathbb{R}^{6N}$. That is, $\boldsymbol{q}_{fast}(t_f)$ remains bounded as $t_f \to \infty$.

Control of the Fast Strain Subdynamics

Proof Sketch 1 (Proof of Theorem 3)

$$\boldsymbol{e}_1 = \theta - \boldsymbol{q}_{fast}^d, \implies \boldsymbol{e}_1' = \theta' - \boldsymbol{q}_{fast}'^d \triangleq \boldsymbol{\nu} - \boldsymbol{q}_{fast}'^d. \tag{25}$$

$$\text{Choose } \boldsymbol{V}_1(\boldsymbol{e}_1) = \frac{1}{2}\boldsymbol{e}_1^\top \boldsymbol{K}_p \boldsymbol{e}_1 \tag{26}$$

$$\text{Then, } \boldsymbol{V}_1' = \boldsymbol{e}_1^\top \boldsymbol{K}_p \boldsymbol{e}_1' = \boldsymbol{e}_1^\top \boldsymbol{K}_p(\boldsymbol{\nu} - \boldsymbol{q}_{fast}'^d). \tag{27}$$

For $\boldsymbol{\nu} = \boldsymbol{q}_{fast}'^d - \boldsymbol{e}_1$, $\boldsymbol{V}_1' = -\boldsymbol{e}_1 \boldsymbol{K}_p \boldsymbol{e}_1 \leq 2\boldsymbol{V}_1$.

Stability Analysis of the Fast Velocity Subdynamics

Theorem 4 (Molu (2024))

Under the tracking error $\boldsymbol{e}_2 = \phi - \boldsymbol{\nu}$ *and matrices* $(\boldsymbol{K}_p, \boldsymbol{K}_q) = (\boldsymbol{K}_p^\top, \boldsymbol{K}_q^\top) > 0$, *the control input*

$$\boldsymbol{u}_{fvel} = \frac{1}{\epsilon}\mathcal{H}_{fast}[\boldsymbol{q}_{fast}^{\prime\prime d} + \boldsymbol{e}_1 - 2\boldsymbol{e}_2 - \boldsymbol{K}_q^\top(\boldsymbol{K}_q\boldsymbol{K}_q^\top)^{-1}\boldsymbol{K}_p\boldsymbol{e}_1] + \frac{1}{\epsilon}\mathcal{H}_{slow}^{fast}\boldsymbol{z}_{slow}^\prime - \boldsymbol{s}_{fast} \tag{28}$$

exponentially stabilizes the fast subdynamics (23).

Stability Analysis of Fast Velocity Subdynamics

Proof Sketch 2 (Sketch Proof of Theorem 4)

Recall from the position dynamics controller:

$$\boldsymbol{e}_1' = \theta' - \boldsymbol{q}_{fast}'^d \triangleq \boldsymbol{z}_{fast} - \boldsymbol{q}_{fast}'^d + (\boldsymbol{\nu} - \boldsymbol{\nu}) \tag{29a}$$

$$= (\phi - \boldsymbol{\nu}) + (\boldsymbol{\nu} - \boldsymbol{q}_{fast}'^d) \triangleq \boldsymbol{e}_2 - \boldsymbol{e}_1. \tag{29b}$$

It follows that

$$\boldsymbol{e}_2' = \phi' - \boldsymbol{\nu}' = \boldsymbol{z}_{fast}' + \boldsymbol{e}_1' - \boldsymbol{q}_{fast}''^d \tag{30}$$

$$= \mathcal{H}_{fast}^{-1}\left[\epsilon \boldsymbol{u}_{fast} + \epsilon \boldsymbol{s}_{fast} - \mathcal{H}_{slow}^{fast} \boldsymbol{z}_{slow}'\right] + (\boldsymbol{e}_2 - \boldsymbol{e}_1) - \boldsymbol{q}_{fast}''^d.$$

Stability Analysis of the Fast Velocity Subdynamics

Proof Sketch 3 (Sketch Proof of Theorem 4)

For diagonal matrices K_p, K_q with positive damping, let us choose the Lyapunov candidate function

$$V_2(\boldsymbol{e}_1, \boldsymbol{e}_2) = \boldsymbol{V}_1 + \frac{1}{2}\boldsymbol{e}_2^\top K_q \boldsymbol{e}_2 = \frac{1}{2}[\boldsymbol{e}_1 \;\; \boldsymbol{e}_2] \begin{bmatrix} K_p & \boldsymbol{0} \\ \boldsymbol{0} & K_q \end{bmatrix} \begin{bmatrix} \boldsymbol{e}_1 \\ \boldsymbol{e}_2 \end{bmatrix}.$$

If $\tilde{\boldsymbol{q}}_{fast} = \boldsymbol{q}_{fast} - \boldsymbol{q}^d_{fast}$ *and* $\tilde{\boldsymbol{q}}'_{fast} = \boldsymbol{q}'_{fast} - \boldsymbol{q}'^d_{fast}$*, then the controller*

$$\boldsymbol{u}_{fvel} = \frac{1}{\epsilon}\mathcal{H}_{fast}[\boldsymbol{q}''^d_{fast} - \tilde{\boldsymbol{q}}_{fast} - 2\tilde{\boldsymbol{q}}'_{fast} - K_q^\top (K_q K_q^\top)^{-1} K_p \tilde{\boldsymbol{q}}_{fast}] + \frac{1}{\epsilon}\mathcal{H}^{fast}_{slow}\boldsymbol{z}'_{slow} - \boldsymbol{s}_{fast},$$

exponentially stabilizes the system;

Stability Analysis of the Fast Velocity Subdynamics

Proof Sketch 4 (Sketch Proof of Theorem 4)

since it can be verified that

$$\begin{aligned} \boldsymbol{V}_2' &= \boldsymbol{e}_1^\top \boldsymbol{K}_p(\boldsymbol{e}_2 - \boldsymbol{e}_1) \\ &\quad - \boldsymbol{e}_2^\top \boldsymbol{K}_q \left(\boldsymbol{e}_2 - \boldsymbol{K}_q^\top (\boldsymbol{K}_q \boldsymbol{K}_q^\top)^{-1} \boldsymbol{K}_p \boldsymbol{e}_1\right) && \text{(31a)} \\ &= -\boldsymbol{e}_1^\top \boldsymbol{K}_p \boldsymbol{e}_1 - \boldsymbol{e}_2^\top \boldsymbol{K}_q \boldsymbol{e}_2 && \text{(31b)} \\ &\triangleq -2\boldsymbol{V}_2 \le 0. && \text{(31c)} \end{aligned}$$

Stability analysis of the slow subdynamics

Set $\boldsymbol{e}_3 = \boldsymbol{z}_{\text{slow}} - \boldsymbol{\nu}$ so that $\dot{\boldsymbol{e}}_3 = \dot{\boldsymbol{z}}_{\text{slow}} - \dot{\boldsymbol{\nu}}$. Then,

$$\dot{\boldsymbol{e}}_3 = \dot{\boldsymbol{z}}_{\text{slow}} - \ddot{\boldsymbol{q}}^d_{\text{fast}} + (\boldsymbol{e}_2 - \boldsymbol{e}_1), \tag{32a}$$

$$= \mathcal{H}^{-1}_{\text{slow}}(\boldsymbol{s}_{\text{slow}} + \boldsymbol{u}_{\text{slow}}) - \ddot{\boldsymbol{q}}^d_{\text{fast}} + (\boldsymbol{e}_2 - \boldsymbol{e}_1). \tag{32b}$$

Theorem 5

The control law

$$\boldsymbol{u}_{slow} = \mathcal{H}_{slow}(\boldsymbol{e}_1 - \boldsymbol{e}_2 - \boldsymbol{e}_3 + \ddot{\boldsymbol{q}}^d_{fast}) - \boldsymbol{s}_{slow} \tag{33}$$

exponentially stabilizes the slow subdynamics.

Stability analysis of the slow subdynamics

Proof.

Consider the Lyapunov function candidate

$$V_3(\boldsymbol{e}_3) = \frac{1}{2}\boldsymbol{e}_3^\top \boldsymbol{K}_r \boldsymbol{e}_3 \text{ where } \boldsymbol{K}_r = \boldsymbol{K}_r^\top > 0. \tag{34}$$

It follows that

$$\dot{V}_3(\boldsymbol{e}_3) = \boldsymbol{e}_3^\top \boldsymbol{K}_r \dot{\boldsymbol{e}}_3 \tag{35a}$$

$$= \boldsymbol{e}_3^\top \boldsymbol{K}_r \left[\mathcal{H}_{\text{slow}}^{-1}(\boldsymbol{s}_{\text{slow}} + \boldsymbol{u}_{\text{slow}}) - \ddot{\boldsymbol{q}}_{\text{fast}}^d + \boldsymbol{e}_2 - \boldsymbol{e}_1\right]. \tag{35b}$$

Substituting $\boldsymbol{u}_{\text{slow}}$ in (33), it can be verified that

$$\dot{V}_3(\boldsymbol{e}_3) = \boldsymbol{e}_3^\top \boldsymbol{K}_r \boldsymbol{e}_3 \triangleq -2V_3(\boldsymbol{e}_3) \leq 0. \tag{36}$$

Hence, the controller (33) stabilizes the slow subsystem. □

Stability of the singularly perturbed interconnected system

Let $\varepsilon = (0,1)$ and consider the composite Lyapunov function candidate $\Sigma(\boldsymbol{z}_{\text{fast}}, \boldsymbol{z}_{\text{slow}})$ as a weighted combination of $\boldsymbol{V}_2$ and $\boldsymbol{V}_3$ i.e. ,

$$\Sigma(\boldsymbol{z}_{\text{fast}}, \boldsymbol{z}_{\text{slow}}) = (1-\varepsilon)\boldsymbol{V}_2(\boldsymbol{z}_{\text{fast}}) + \varepsilon \boldsymbol{V}_3(\boldsymbol{z}_{\text{slow}}),\; 0 < \varepsilon < 1. \tag{37}$$

It follows that,

$$\begin{aligned}\dot{\Sigma}(\boldsymbol{z}_{\text{fast}}, \boldsymbol{z}_{\text{slow}}) &= (1-\varepsilon)[\boldsymbol{e}_1^\top \boldsymbol{K}_p \dot{\boldsymbol{e}}_1 + \boldsymbol{e}_2^\top \boldsymbol{K}_q \dot{\boldsymbol{e}}_2] + \varepsilon \boldsymbol{e}_3^\top \boldsymbol{K}_r \dot{\boldsymbol{e}}_3, \\ &= -2(\boldsymbol{V}_2 + \boldsymbol{V}_3) + 2\varepsilon \boldsymbol{V}_2 \le 0 \end{aligned} \tag{38}$$

which is clearly negative definite for any $\varepsilon \in (0,1)$. Therefore, we conclude that the origin of the singularly perturbed system is asymptotically stable under the control laws.

$$\boldsymbol{u}(\boldsymbol{z}_{\text{fast}}, \boldsymbol{z}_{\text{slow}}) = (1-\varepsilon)\boldsymbol{u}_{\text{fast}} + \varepsilon \boldsymbol{u}_{\text{slow}}. \tag{39}$$

Asynchronous, time-separated control

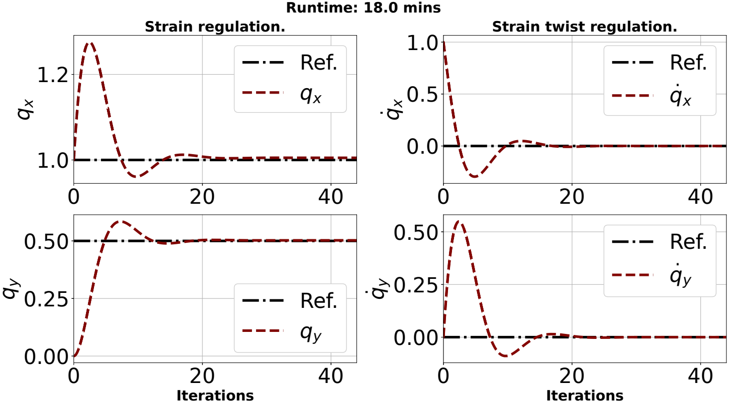

Ten discretized PCS sections: 6 fast, 4 slow subsections. $\mathcal{F}_p^y = 10\,N$, with $K_p = 10$, $K_d = 2.0$ for $\eta^d = [0, 0, 0, 1, 0.5, 0]^\top$ and $\xi^d = \mathbf{0}_{6\times 1}$.

Five-axes control

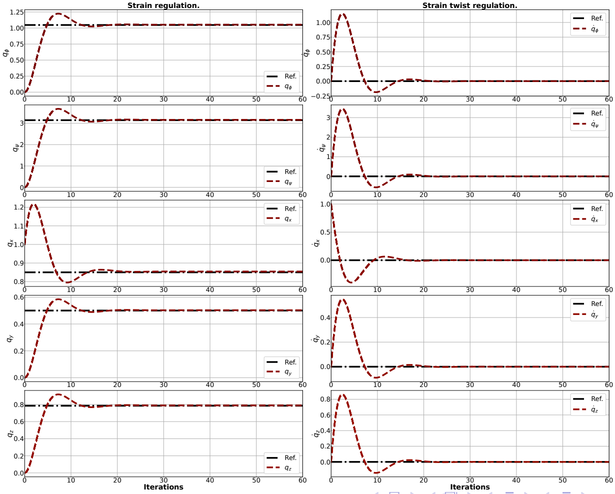

Time Response Comparison with Non-hierarchical Controller

Pieces			Runtime (mins)	
Total	Fast	Slow	Hierarchical SPT (mins)	Single-layer PD control (hours)
6	4	2	18.01	51.46
8	5	3	30.87	68.29
10	7	3	32.39	107.43

Table: Time to Reach Steady State.

Contributions

- Layered singularly perturbed techniques for decomposing system dynamics to multiple timescales.
- Stabilizing nonlinear backstepping controllers were introduced to the respective subdynamics for fast strain regulation.

Discussions

- Leverage the *multiphysics of (often) heterogeneous soft material components*;
- Neat manipulation strategies for motion is a *multiscale problem* that requires imbuing geometric mathematical reasoning into the control strategies for desired movements.
- Challenge: Merging the long-term planning horizon of spatial perception tasks with the *fast time-constant* (typically milliseconds or microseconds) requirements of the precise control of soft, compliant pneumatic/mechanical systems across multiple time-scales;

Discussions

- Process spatial information (Lagrangian) often within a long-time horizon context (Eulerian) for the real-time control or planning across multiple time-scales.

Conclusion

- Email: lekanmolu@microsoft.com
- Thank you!

References I

Cosimo Della Santina, Christian Duriez, and Daniela Rus. Model-based control of soft robots: A survey of the state of the art and open challenges. *IEEE Control Systems Magazine*, 43(3):30–65, 2023. doi: 10.1109/MCS.2023.3253419.

Derek E Moulton, Thomas Lessinnes, and Alain Goriely. Morphoelastic Rods III: Differential Growth and Curvature Generation in Elastic Filaments. *Journal of the Mechanics and Physics of Solids*, 142:104022, 2020.

Bartosz Kaczmarski, Alain Goriely, Ellen Kuhl, and Derek E Moulton. A Simulation Tool for Physics-informed Control of Biomimetic Soft Robotic Arms. *IEEE Robotics and Automation Letters*, 2023.

Mattia Gazzola, LH Dudte, AG McCormick, and Lakshminarayanan Mahadevan. Forward and inverse problems in the mechanics of soft filaments. *Royal Society open science*, 5(6):171628, 2018.

M. B. Rubin. *Cosserat Theories: Shells, Rods, and Points*. Springer-Science+Business Medis, B.V., 2000.

Eugène Maurice Pierre Cosserat and François Cosserat. *Théorie des corps déformables*. A. Hermann et fils, 1909.

Isuru S Godage, David T Branson, Emanuele Guglielmino, Gustavo A Medrano-Cerda, and Darwin G Caldwell. Shape function-based kinematics and dynamics for variable length continuum robotic arms. In *2011 IEEE International Conference on Robotics and Automation*, pages 452–457. IEEE, 2011.

Robert J. III Webster and Bryan A. Jones. Design and kinematic modeling of constant curvature continuum robots: A review. *The International Journal of Robotics Research*, 29(13):1661–1683, 2010.

Ke Qiu, Jingyu Zhang, Danying Sun, Rong Xiong, Haojian Lu, and Yue Wang. An efficient multi-solution solver for the inverse kinematics of 3-section constant-curvature robots. *arXiv preprint arXiv:2305.01458*, 2023.

Federico Renda, Vito Cacucciolo, Jorge Dias, and Lakmal Seneviratne. Discrete cosserat approach for soft robot dynamics: A new piece-wise constant strain model with torsion and shears. *IEEE International Conference on Intelligent Robots and Systems*, 2016-Novem:5495–5502, 2016. ISSN 21530866.

References II

Federico Renda, Frédéric Boyer, Jorge Dias, and Lakmal Seneviratne. Discrete cosserat approach for multisection soft manipulator dynamics. *IEEE Transactions on Robotics*, 34(6):1518–1533, 2018.

Federico Renda, Michele Giorelli, Marcello Calisti, Matteo Cianchetti, and Cecilia Laschi. Dynamic model of a multibending soft robot arm driven by cables. *IEEE Transactions on Robotics*, 30(5):1109–1122, 2014.

José Guadalupe Romero, Romeo Ortega, and Ioannis Sarras. A globally exponentially stable tracking controller for mechanical systems using position feedback. *IEEE Transactions on Automatic Control*, 60(3):818–823, 2014.

Lekan Molu and Shaoru Chen. Lagrangian Properties and Control of Soft Robots Modeled with Discrete Cosserat Rods. In *IEEE International Conference on Decision and Control, Milan, Italy*. IEEE, 2024.

Nikolai Matni, Aaron D Ames, and John C Doyle. A quantitative framework for layered multirate control: Toward a theory of control architecture. *IEEE Control Systems Magazine*, 44(3):52–94, 2024.

Lekan Molu. Fast Whole-Body Strain Regulation in Continuum Robots. *(submitted to) American Control Conference*, 2024.

Gianmarco Mengaldo, Federico Renda, Steven L Brunton, Moritz Bächer, Marcello Calisti, Christian Duriez, Gregory S Chirikjian, and Cecilia Laschi. A concise guide to modelling the physics of embodied intelligence in soft robotics. *Nature Reviews Physics*, 4(9):595–610, 2022.